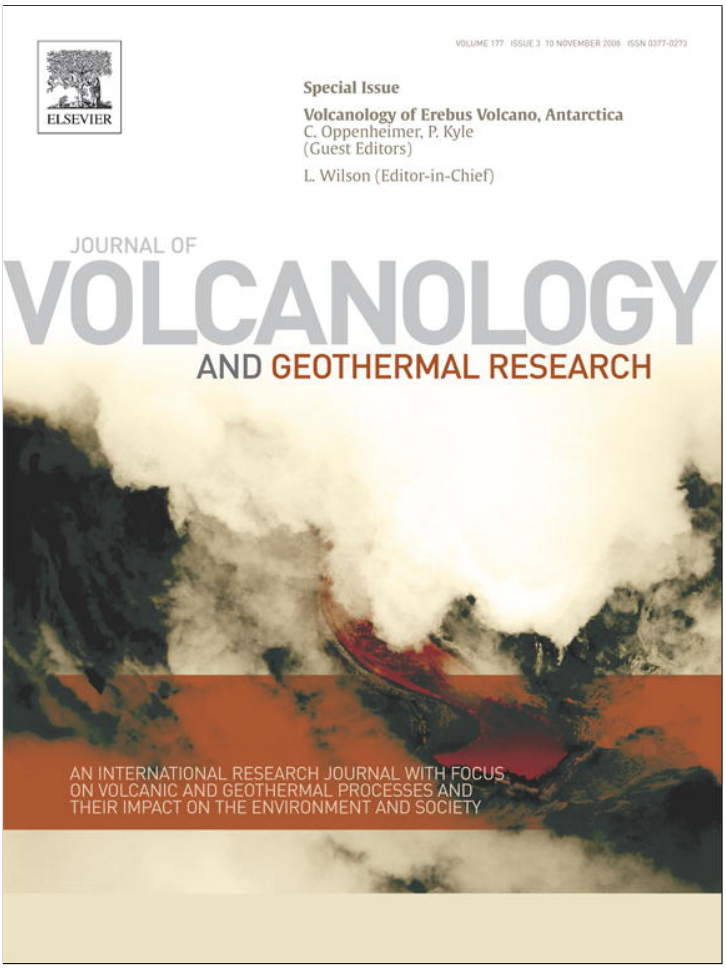

Journal of Volcanology and Geothermal Research 177 (2008) 606–618

Contents lists available at ScienceDirect

Journal of Volcanology and Geothermal Research

journal homepage: www.elsevier.com/locate/jvolgeores

A Sr, Nd, Hf, and Pb isotope perspective on the genesis and long-term evolution of alkaline magmas from Erebus volcano, Antarctica

Kenneth W.W. Sims [a,*], Janne Blichert-Toft [b], Philip R. Kyle [c], Sylvain Pichat [a,b], Pierre-Jean Gauthier [d], Jurek Blusztajn [a], Peter Kelly [c,e], Lary Ball [f], Graham Layne [a,g]

[a] Department of Geology and Geophysics, Woods Hole Oceanographic Institution, Woods Hole, MA 02543, United States
[b] Ecole Normale Supérieure, CNRS UMR 5570, 46 Allée d'Italie, 69364 Lyon, France
[c] Department of Earth and Environmental Science, New Mexico Institute of Mining and Technology, Socorro, NM 87801-4796, United States
[d] Laboratoire Magmas et Volcans-Observatoire de Physique du Globe de Clermont-Ferrand (CNRS, UBP)-5 rue Kessler-63000 Clermont-Ferrand, France
[e] Climate Change Research Center, University of New Hampshire, Durham, NH 03824, United States
[f] Department of Marine Chemistry and Geochemistry, Woods Hole Oceanographic Institution, Woods Hole, MA 02543, United States
[g] Memorial University INCO Innovation Centre, IIC 1047 St. John's, Canada NL A1B 3X5

ARTICLE INFO

Article history:
Available online 28 August 2007

Keywords:
long-lived radiogenic isotopes
Mt. Erebus
alkaline volcanism
mantle sources
HIMU mantle source
Antarctic Volcanism

ABSTRACT

We report new Nd, Hf, Sr, and high-precision Pb isotopic data for 44 lava and tephra samples from Erebus volcano. The samples cover the entire compositional range from basanite to phonolite and trachyte, and represent all three phases of the volcanic evolution from 1.3 Ma to the present. Isotopic analyses of 7 samples from Mt. Morning and the Dry Valley Drilling Project (DVDP) are given for comparison. The Erebus volcano samples have radiogenic $^{206}Pb/^{204}Pb$, unradiogenic $^{87}Sr/^{86}Sr$, and intermediate $^{143}Nd/^{144}Nd$ and $^{176}Hf/^{177}Hf$, and lie along a mixing trajectory between the two end-member mantle components DMM and HIMU. The Erebus time series data show a marked distinction between the early-phase basanites and phonotephrites, whose Nd, Hf, Sr, and Pb isotope compositions are variable (particularly Pb), and the current 'phase-three' evolved phonolitic lavas and bombs, whose Nd, Hf, Sr, and Pb isotope compositions are essentially invariant. Magma mixing is inferred to play a fundamental role in establishing the isotopic and compositional uniformity in the evolved phase-three phonolites. In-situ analyses of Pb isotopes in melt inclusions hosted in an anorthoclase crystal from a 1984 Erebus phonolite bomb and in an olivine from a DVDP basanite are uniform and identical to the host lavas within analytical uncertainties. We suggest that, in both cases, the magma was well mixed at the time melt inclusions were incorporated into the different mineral phases.

1. Introduction

Erebus volcano, Antarctica, offers an unprecedented opportunity to study the genesis and evolution of alkaline magmas for several reasons. First, its lavas and tephras span a wide compositional range from primitive basanite to evolved, anorthoclase-rich phonolite (Kyle et al., 1992). Second, its persistent Strombolian activity has ejected bombs from the lava lake on to the crater rim and thus provided samples to examine the magma compositions from 1972 until the present day. Third, the well-dated lava sequence provides a temporal record ranging from 1.3 Ma to the present and shows the longer term evolution of the volcano (Harpel et al., 2004; Esser et al., 2004).

Only few measurements of the long-lived radiogenic isotopes exist for samples from Erebus volcano and surrounding areas. By contrast, there are several detailed and comprehensive geochemical studies that examine the genesis and evolution of the lavas, tephras, and gases at Erebus (Kyle et al., 1992; Caldwell and Kyle, 1994; Zreda-Gostynska et al., 1997; Ryan and Kyle, 2004; Harpel et al., 2007-this volume; Kelly et al., 2007-this volume-a,b; Oppenheir et al., 2007-this volume; Sims et al., 2007-this volume). The existing, albeit limited, radiogenic isotopic data provide important constraints on the significant HIMU component in the source of magmas on Ross Island and surroundings (Sun and Hanson, 1975; Kyle et al., 1992; Rocholl et al., 1995; Sims and Hart, 2006). However, without a more comprehensive study of the isotopic compositions of Erebus lavas and pyroclastic rocks it is not possible to establish the relative influences of source versus process during the genesis and evolution of the various magmatic lineages.

In this study we present Nd, Hf, Sr, and high-precision Pb isotopic analyses of 44 samples from Erebus volcano, 3 samples from Mt. Morning, and 4 drill core samples from the Dry Valley Drilling Project (DVDP) (Kyle, 1981). The Erebus samples span several magmatic lineages and include samples from all three phases of the 1.3 Ma to present evolutionary history of Erebus volcano (Esser et al., 2004). We also report in-situ measurements of Pb isotopes in melt inclusions hosted in an anothoclase crystal from a phonolite bomb erupted in

* Corresponding author.
E-mail address: ksims@whoi.edu (K.W.W. Sims).

0377-0273/$ – see front matter © 2007 Elsevier B.V. All rights reserved.
doi:10.1016/j.jvolgeores.2007.08.006

Table 1
Nd, Sr, Hf, and Pb isotope compositions of DVDP and Mt. Morning lavas and Erebus volcano lavas and bombs. The Erebus bombs were collected either in the Erebus crater or on its summit cone. The lavas were collected along the Erebus flanks and their locations and ages are given in (Esser et al., 2004; Harpel et al., 2004; Kelly et al., 2007-this volume-b)

Sample	Rock type[a]	Year/age	$^{87}Sr/^{86}Sr$	$^{143}Nd/^{144}Nd$	ε_{Nd}	$^{176}Hf/^{177}Hf$	ε_{Hf}	$^{206}Pb/^{204}Pb$	$^{207}Pb/^{204}Pb$	$^{208}Pb/^{204}Pb$
Historic bombs										
25724[b,c]	Phono.	1972	0.703058	0.512911	5.3	0.282971	7.0	19.953	15.653	39.524
25721[b,c]	Phono.	1974	0.703019	0.512900	5.1	0.282949	6.3	19.948	15.650	39.519
2E2[b,c]	Phono.	1974	0.703021			0.282955	6.5			
[B][d,e]			0.703024	0.512101	5.2					
[L1][d,f]						0.282962	6.7	19.947	15.652	39.500
[L2][d,f]								19.944	15.649	39.506
25723[b,c]	Phono.	1975	0.703019	0.512886	4.8	0.282964	6.8	19.944	15.649	39.513
77016[b,c]	Phono.	1977	0.703039	0.512905	5.2	0.282954	6.4	19.949	15.649	39.517
78325[b,c]	Phono.	1977	0.703031	0.512887	4.9	0.282942	6.0	19.948	15.649	39.515
79302[b,c]	Phono.	1979	0.703033	0.512925	5.6	0.282951	6.3	19.945	15.650	39.512
80300[b,c]	Phono.	1980	0.703038	0.512924	5.6	0.282936	5.8	19.952	15.653	39.508
81401[b,c]	Phono.	1981	0.703024	0.512906	5.2	0.282938	5.9	19.947	15.649	39.515
82416[b,c]	Phono.	1982		0.512891	4.9	0.282954	6.4	19.946	15.650	39.519
[L1][d]						0.282953	6.4			
83220[b,c]	Phono.	1983	0.703039	0.512908	5.3	0.282963	6.8	19.946	15.649	39.515
[L1]						0.282963	6.7			
84501[b,c]	Phono.	1984	0.703102	0.512916	5.4	0.282958	6.6	19.916	15.648	39.489
[L1][d]								19.897	15.654	39.486
84500[b,c]	Phono.	1984	0.703109	0.512898	5.1	0.282961	6.7	19.929	15.647	39.491
84505[b,c]	Phono.	1984	0.703079	0.512910	5.3	0.282947	6.2			
[B][d,e]			0.703082	0.512103	5.2					
[L1][d,f]								19.920	15.648	39.492
85009[b,c]	Phono.	1985	0.703061	0.512904	5.2	0.282959	6.6	19.941	15.647	39.507
85010[b,c]	Phono.	1985	0.703036	0.512904	5.2	0.282951	6.3			
86022[b,c]	Phono.	1986	0.703022	0.512924	5.6	0.282965	6.8	19.944	15.649	39.513
89001[b,c]	Phono.	1989	0.703021	0.512930	5.7	0.282946	6.2	19.947	15.649	39.517
91101[b,c]	Phono.	1991	0.703026	0.512929	5.7	0.282943	6.0	19.937	15.646	39.506
Er92KS[b,c]	Phono.	1992	0.703035	0.512912	5.3	0.282952	6.4	19.946	15.650	39.516
[B][d,e]			0.703028	0.512108	5.3					
[L1][d,f]						0.282948	6.2	19.959	15.665	39.525
93102[b,c]	Phono.	1993	0.703022	0.512906	5.2	0.282952	6.4	19.944	15.648	39.505
[L1][d,f]								19.945	15.648	39.508
[L2][d,f]								19.943	15.648	39.504
Er96[b,c]	Phono.	1996	0.703026	0.512906	5.2	0.282942	6.0	19.941	15.648	39.505
Er97[b,c]	Phono.	1997	0.703033	0.512911	5.3	0.282935	5.8	19.940	15.648	39.509
[L][d,f]								19.935	15.640	39.507
Er99[b,c]	Phono.	1999	0.703042	0.512910	5.3	0.282960	6.6	19.937	15.646	39.505
[L1][d,f]								19.935	15.645	39.500
[L2][d,f]								19.939	15.647	39.507
Er2000[b,c]	Phono.	2000	0.703043	0.512905	5.2	0.282957	6.5	19.939	15.648	39.508
Er2001[b,c]	Phono.	2001	0.703018	0.512903	5.2	0.282955	6.5	19.923	15.650	39.498
Jan 2004[b,c]	Phono.	2004	0.703051	0.512903	5.2	0.282962	6.7	19.943	15.651	39.515
Dec-05[b,c]	Phono.	2005	0.703010	0.512891	4.9	0.282968	6.9			
Stage-3 EL phonolite lavas										
E83452[b,c]	Phono.	23±3 ka	0.703017	0.512931	5.7	0.282962	6.7	19.976	15.659	39.551
E87066[b,c]	Phono.	17±8 ka	0.703077	0.512927	5.6	0.282955	6.5	19.957	15.649	39.522
E87030[b,c]	Phono.	13±2 ka		0.512900	5.1	0.282965	6.8			
E87085[b,c]	Phono.	12±3 ka	0.703088	0.512872	4.6	0.282965	6.8	19.963	15.651	39.531
E87020[b,c]	Phono.	11±6 ka	0.703085	0.512909	5.3	0.282963	6.8	19.957	15.649	39.519
E87034[b,c]	Phono.	11±8 ka	0.703025	0.512928	5.7	0.282943	6.1	19.968	15.658	39.544
E87035[b,c]	Phono.	10±5 ka		0.512928	5.7	0.282948	6.2	19.962	15.654	39.535
E87004[b,c]	Phono.	9±2 ka	0.703088	0.512912	5.3	0.282949	6.3	19.996	15.673	39.610
E87054[b,c]	Phono.	9±7 ka		0.512894	5.0	0.282946	6.2	19.958	15.649	39.522
Stage-3 El phonolite lavas										
E87083[b,c]	Phono.	6±2 ka	0.703005	0.512904	5.2	0.282947	6.2	19.975	15.657	39.548
E87051[b,c]	Phono.	4±3 ka	0.703008	0.512904	5.2	0.282952	6.4	19.963	15.652	39.530
E87040[b,c]	Phono.	0±4 ka	0.703017	0.512923	5.6	0.282963	6.8	19.993	15.671	39.600
Stage-1 EL lavas										
EL 83432[b,c,g]	Basanite	1.311 Ma	0.702922	0.512886	4.8	0.282978	7.3	20.006	15.666	39.701
EL 83437[b,c,g]	Basanite	1.311 Ma	0.702969	0.512927	5.6	0.282962	6.7			
DVDP-2 lavas										
DVDP 2–45.86[b,c]	Te-Phon.	1.2 Ma	0.703021	0.512905	5.2	0.282924	5.4	19.629	15.638	39.206
DVDP 2–61.23[b,c]	Te-Phon.	1.2 Ma	0.703040	0.512884	4.8	0.282924	5.4	20.278	15.702	39.866
DVDP 2–76.38[b,c]	Phon-Te.	1.2 Ma	0.703081	0.512877	4.7	0.282932	5.7	20.174	15.663	39.724
DVDP 2–105.53[b,c]	Basanite	1.25 Ma	0.702991	0.512929	5.7	0.282944	6.1	19.496	15.666	39.069
Enriched Fe-series										
AW82015[b,c,g]	Te-Phon.	243±10 ka	0.703034	0.512912	5.3	0.282952	6.4			
Ice-station[b,c,g]	Trachyte	159±2 ka	0.704251	0.512916	5.4	0.282923	5.3	19.366	15.643	39.129

(continued on next page)

Table 1 *(continued)*

Sample	Rock type[a]	Year/age	$^{87}Sr/^{86}Sr$	$^{143}Nd/^{144}Nd$	ε_{Nd}	$^{176}Hf/^{177}Hf$	ε_{Hf}	$^{206}Pb/^{204}Pb$	$^{207}Pb/^{204}Pb$	$^{208}Pb/^{204}Pb$
MT Morning										
MM-01A SP-02[b,c]	Basanite	~20 ka	0.703226	0.512840	3.9	0.282932	5.7	19.835	15.655	39.575
MM-02A GPS-02[b,c]	Basanite	~20 ka	0.703314	0.512902	5.2	0.282951	6.3	19.971	15.650	39.632
MM-01A[b,c]	Basanite	~20 ka	0.703314	0.512882	4.8	0.282956	6.5	19.884	15.662	39.590

[a] Samples are categorized using the chemical classification based on the total alkali-silica diagram of LeBas et al. (1986). Rock type abbreviations: Phono — Phonolite; Te-Phon — Tephraphonolite; Phon-Te — Phonotephrite.

[b] All Pb, Sr and Nd isotopes measured at WHOI by PIMMS using the ThermoFinnigan NEPTUNE unless indicated by replicate designators [L1], [L2] or [B] in sample label column. For Sr and Nd the internal precision is 5–10 ppm (2s); external precision after adjusting to 0.71024 (NBS SRM 987) and 0.511847 (La Jolla Nd standard), respectively, is estimated to be 15–30 ppm. ε_{Nd} values calculated using $(^{143}Nd/^{144}Nd)_{Chur(0)}=0.512638$. Pb analyses have internal precisions of xxx/204 of 15–30 ppm; SRM 997 Tl was used as an internal standard, and then normalized to NBS 981 using the values of Todt et al. (1996). External reproducibility (including full chemistry) for $^{208}Pb/^{204}Pb$, $^{207}Pb/^{204}Pb$, and $^{206}Pb/^{204}Pb$ are 150–200 ppm (2σ) and 90 ppm (2σ) for $^{208}Pb/^{206}Pb$. To verify reproducibility for Pb isotopic measurements we analyzed two USGS standards AGV-1 and BCR-1. The average of AGV-1 was $^{206}Pb/^{204}Pb=18.9414$, $^{207}Pb/^{204}Pb=15.6548$, $^{208}Pb/^{204}Pb=38.5615$; BCR-1 $^{206}Pb/^{204}Pb=18.8215$, $^{207}Pb/^{204}Pb=15.6356$, $^{208}Pb/^{204}Pb-38.7309$. Further details can be found in Hart et al. (2004, 2005) and Hart and Blusztajn (2006).

[c] All Hf isotopes measured at ENS Lyon by PIMMS using the VG Plasma 54 (Blichert-Toft et al., 1997). Uncertainties on measured Hf isotope ratios based on in-run analytical errors ($2\sigma/\sqrt{n}$, where n is the number of measured ratios) are less than ±30 ppm. Measured ratios are normalized for mass fractionation to $^{179}Hf/^{177}Hf=0.7325$. Measurement of $^{176}Hf/^{177}Hf$ in the JMC-475 Hf isotopic standard = 0.28216 ± 1. ε_{Hf} values calculated with $(^{176}Hf/^{177}Hf)$ Chur (0) = 0.282772 (Blichert-Toft and Albarède, 1997). Hf isotope replicates are designated by [L1] in sample label column.

[d] Separate powder replicates designated as [B] for the Sr and Nd isotopes measured at UC Berkeley, and [L1] and [L2] for the Hf and Pb replicates measured at ENS Lyon.

[e] Nd and Sr isotope replicates measured at UC Berkeley by TIMS using a VG 354 and are designated by [B] in sample label column. Nd isotope measurements are normalized to $^{146}Nd/^{144}Nd=0.636151$. ε_{Nd} values calculated using $(^{143}Nd/^{144}Nd)Chur(0)=0.511831\pm17$ for BCR-1 (measured values at UC Berkeley). Measurement errors based on in run statistics are less than 20 ppm.

[f] Pb isotope replicates measured at ENS Lyon by PIMMS using the VG Plasma 54 and are designated by [L1] or [L2] in sample label column. Measured ratios are normalized to both an internal Tl std and then to NBS 981 using the values of (Todt et al., 1996). For these measurements every two samples are interspersed with analyses of NBS 960 for the mass bias correction (see White et al., 2000). Errors for $^{208}Pb/^{204}Pb$, $^{207}Pb/^{204}Pb$, and $^{206}Pb/^{204}Pb$ are 150–200 ppm (2σ) and for $^{208}Pb/^{206}Pb$ 100–200 ppm (2σ) and are calculated by propagating ($\sqrt{(se^2+se^2)}$) both the analytical error and the variance of the NBS 960 standards from the instrument fractionation trend observed during the sum of these analyses.

[g] Results for $^{87}Sr/^{86}Sr$ analyses measured by TIMS from Kyle et al. (1992) for samples AW82015 (0.703027), 83432 (0.702937) and 83437 (0.702977) agree within analytical uncertainties. Although the samples are not replicated directly, the Kyle et al. Nd isotope measurement for the anorthoclase phonolite sample ($\varepsilon_{Nd}=5.3$) from Three Sisters agrees well with our other measurements of upper slope anorthoclase phonolite lavas. Similarly, the Aurora Cliffs trachyte sample has a $^{87}Sr/^{86}Sr$ (0.704248) similar to the Ice-Station trachyte measured in this study.

1984 and in olivines from a DVDP basanite. A representative and primitive DVDP basanite is used as the parental composition to model magmatic evolution of both the DVDP and Erebus lineages. The new radiogenic isotope data presented here combined with the corresponding major and trace element compositions (Kyle, 1981; Kyle et al., 1992; Kelly et al., 2007-this volume-a) provide constraints on the mantle source of the parental Erebus magmas and the magmatic evolution of the Erebus lavas from 1.3 Ma to the present.

2. Background on Erebus volcano

The geology of Erebus volcano is thoroughly described elsewhere (Moore and Kyle, 1987, 1990; Kyle, 1990a,b, 1992; Esser et al., 2004; Harpel et al., 2004; Kelly et al., 2007-this volume-a) and only the most pertinent aspects are summarized here. Erebus is an active composite volcano and is the largest of four volcanic centers forming Ross Island: *Mt. Erebus* (3794 m elevation, 2170 km^3), *Mt. Terror* (3262 m, 1700 km^3), *Mt. Bird* (1800 m, 470 km^3), and *Hut Point Peninsula* (100 km^3). About 4520 km^3 of volcanic material has been erupted on Ross Island over the last ~4 Ma (Esser et al., 2004). Ross Island overlies thin (17–25 km) rifted continental crust at the southern terminus of the Terror Rift, which is a major graben located at the western margin of the West Antarctic rift system (Cooper et al., 1987; Behrendt et al., 1991; Behrendt, 1999; Bannister et al., 2000). Late Cenozoic, intraplate, silica-undersaturated, alkaline volcanics erupted on the western margin of the Ross Embayment belong to the McMurdo Volcanic Group (MVG) (Kyle, 1990a). In the southern Ross Sea and McMurdo Sound the MVG is referred to as the Erebus volcanic province (Kyle, 1990b).

High-precision $^{40}Ar/^{39}Ar$ dating (Esser et al., 2004; Harpel et al., 2004) has divided the history of Mt. Erebus into three distinct phases: 1) The proto-Erebus shield building phase (1.3–1.0 Ma), during which basanites were erupted; 2) the proto-Erebus cone building phase (1.0 Ma–250 ka), dominated by more evolved phonotephrite lavas forming the steep slopes of the volcano; and 3) the modern-Erebus cone building phase (250 ka-present), when activity increased and large volumes of anorthoclase–phyric tephriphonolite and phonolite lavas were extruded. Minor trachyte was also erupted at about 170 ka during the third phase of activity.

Erebus volcano has hosted a persistent convecting and degassing lava lake of anorthoclase–phyric phonolite magma for at least 35 years. All historic eruptive activity has originated from this phonolite lava lake and adjacent vents, which were first observed directly by a scientific party in December 1972 (Giggenbach et al., 1973; Kyle et al., 1982). Variations in the style and magnitude of volcanic activity between 1972 and early 2006 include a period of larger and more frequent Strombolian eruptions in 1984 (Kyle, 1986; Caldwell and Kyle, 1994), a phreatic eruption in 1993, and a period of almost no eruptions from 2002 to 2004. Since mid-2005 there has been a return to more frequent Strombolian activity.

Lavas on Ross Island show two major magmatic lineages, the DVDP lineage, named after samples from the Dry Valley Drilling Project (Kyle, 1981), and the Erebus Lineage (EL) (Kyle et al., 1992). The DVDP lineage lavas are older and occur at the volcanic centers surrounding Erebus volcano (*Mt. Terror*, *Mt. Bird*, and *Hut Point Peninsula*). They consist predominantly of basanite with minor microporphyritic kaersutite-bearing intermediate differentiates and phonolite. The Erebus lineage constitutes a surprisingly simple (Kyle et al., 1992) and coherent fractionation trend, defined by a single liquid-line of descent from basanite to phonolite with a complete sequence of intermediate (phonotephrite, tephriphonolite) eruptive products. Minor volumes of more iron-rich and less silica undersaturated benmoreite and trachytes, termed the enriched Fe series (EFS), occur as isolated outcrops on the flanks of Erebus and adjacent islands in Erebus Bay. The EFS lavas follow a different liquid-line of descent and the trachytes are interpreted to have undergone both assimilation and fractional crystallization during their evolution.

There are surprisingly few measurements of the isotopic compositions of lavas from Ross Island and Erebus volcano and these limited older data are of inferior quality compared to modern analyses. Marie Byrd Land, on the eastern flank of the West Antarctic Rift System, has yielded a number of studies on the isotopic characteristics of the alkalic lavas (Futa and LeMasurier, 1983; Hart et al., 1995, 1997; Panter et al., 2000; Rocchi et al., 2002; Panter et al., 2006). Stuckless and Ericksen (1976) report low-precision Sr isotopic data on samples from the Erebus volcanic province, including a few samples from DVDP cores. Sun and Hanson (1975) measured Pb isotopes by thermal ionization mass spectrometry (TIMS) in a limited number of basanites

and related differentiates from the Erebus volcanic province. They noted a unique "HIMU" or radiogenic Pb isotopic signature for the MVG lavas, which has since turned out to be a seemingly ubiquitous characteristic of Antarctic and Southwest Pacific Cenozoic volcanism (Rocholl et al., 1995; Hart et al., 1995, 1997; Finn et al., 2005, Panter et al., 2006). Kyle et al. (1992) measured Sr isotopes for several samples from the EL and EFS suites. They concluded that the uniform Sr isotopes from basanite to phonolite supported major-element modeling, which indicates that the EL resulted from simple fractional crystallization of a parental basanite derived from a homogeneous mantle source. The high $^{87}Sr/^{86}Sr$ of the trachyte indicates that assimilation of continental crust was involved in the evolution of the EFS. Sims and Hart (2006) reported Nd, Sr, Th, and Pb isotopes on four historic bombs as part of a global study evaluating the relationship between U–Th disequilibria systematics and long-lived radiogenic Nd, Sr, and Pb isotope systematics.

The samples analyzed in this study come from all three eruptive phases of Erebus volcano and cover the basanite to phonolite compositional range, which defines the EL. A single trachyte sample represents the EFS. Four samples characteristic of the DVDP lineage are provided for comparison. Specific emphasis was given to analyzing the DVDP and early phase-one EL samples, which are used as parental end-members for calculating the liquid-line of descent for the EL (Kyle et al., 1992) and the dated upper summit phonolite lavas (Esser et al., 2004) and historic phonolite bombs collected over the past 30 years. The major and trace element compositions of these samples have been previously characterized and are reported elsewhere (Kyle, 1981; Kyle et al., 1992; Kelly et al., 2007-this volume-a,b).

3. Results

3.1. Radiogenic isotopes: Sr, Nd, Hf, and Pb

Sr, Nd, Hf, and high-precision Pb isotopes were measured for: 1) a suite of 28 historic phonolite bombs spanning the time interval from 1974 to 2005; 2) 13 dated surface flows from the upper flanks of Erebus volcano; 3) four samples from the DVDP lineage; 4) one dated trachyte sample from the lower flanks of Erebus; and 5) three dated lava flows from the nearby Mt. Morning. The isotopic data are listed in Table 1 and shown in Figs. 1–7.

Nd, Sr, and Pb isotopes were measured at WHOI using the Thermo Finnigan Neptune Plasma ionization multi-collector mass spectrometer (PIMMS). Hf and Pb isotopes were measured at the Ecole Normale Supérieure in Lyon (ENSL), France, using the VG Plasma 54

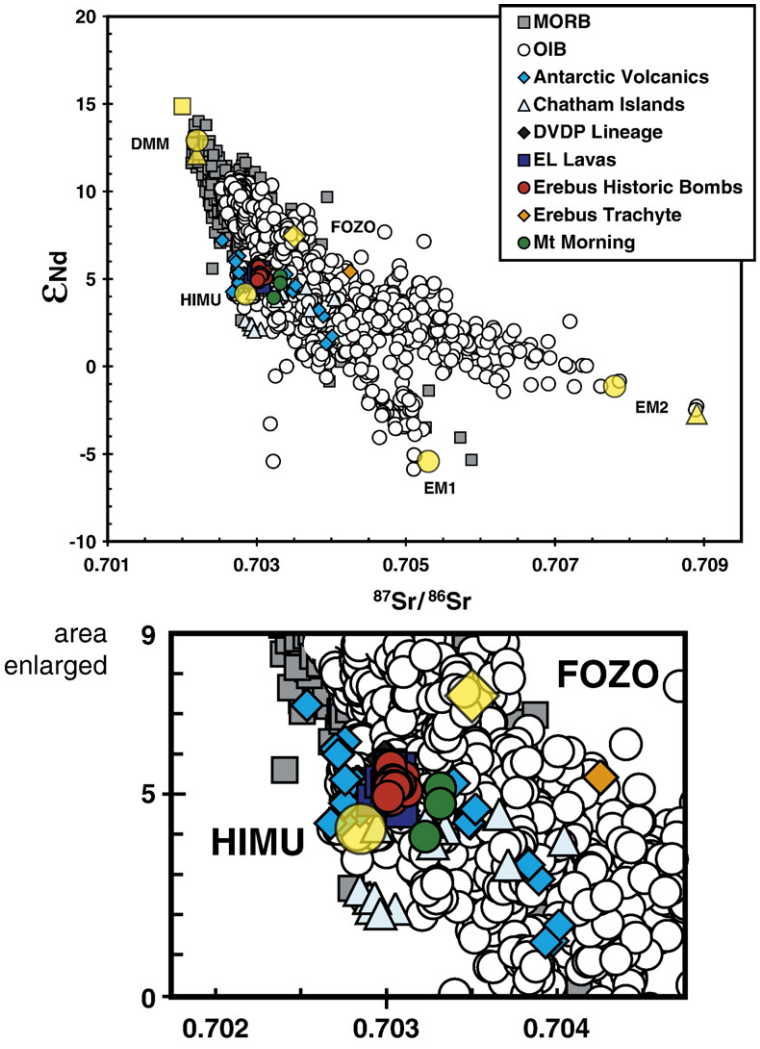

Fig. 1. ε_{Nd} versus $^{87}Sr/^{86}Sr$ for Erebus volcano, DVDP lineage, and Mt. Morning samples analyzed in this study. Also shown are the existing Nd and Sr isotope data from West Antarctic volcanics (Hart et al., 1995, 1997; Panter et al., 2000) and the Chatham Islands (Panter et al., 2006), as well as a compilation of the MORB-OIB data base from Stracke et al. (2003, 2005) and Agranier et al. (2005). End-member mantle components are from Zindler and Hart (1986) (yellow circles); Workman et al. (2004) (EM2: yellow triangle); Salters and Stracke (2004) (DMM: yellow square), Workman and Hart (2005) (DMM: yellow triangle), and Hart et al. (1992) (FOZO: yellow triangle). Enlarged area focuses on the Antarctic data set.

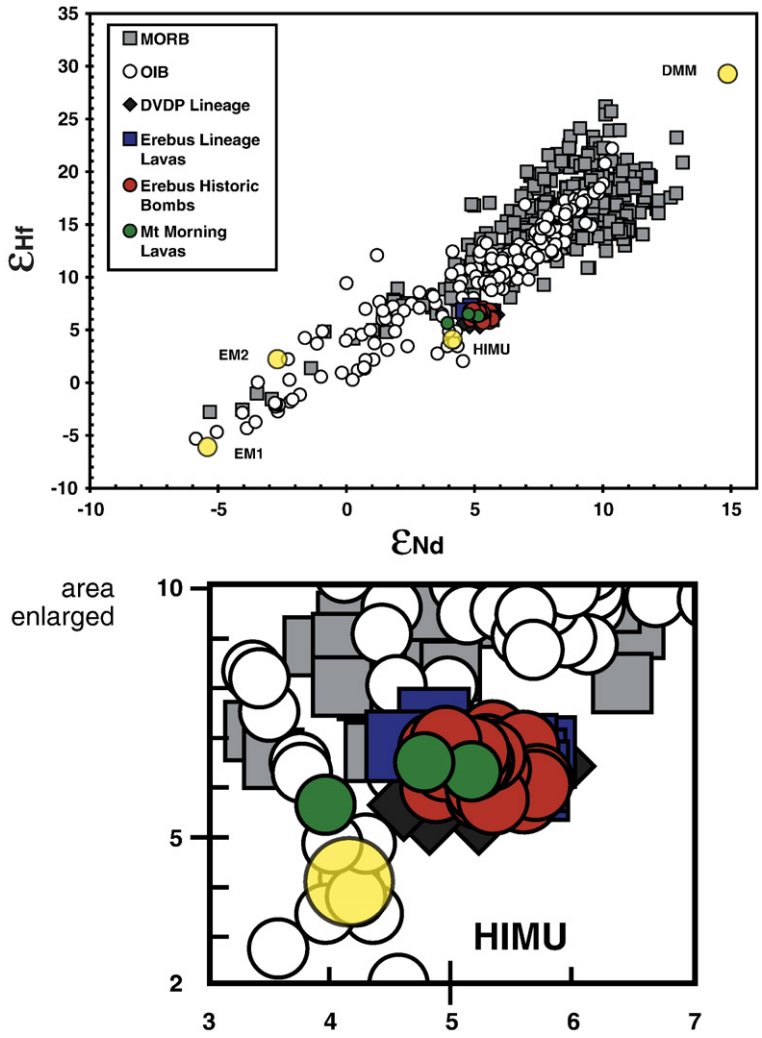

Fig. 2. ε_{Nd} versus ε_{Hf} for Erebus volcano, DVDP lineage, and Mt. Morning samples analyzed in this study. To our knowledge there are no previous measurements of Hf isotopes for Antarctic samples. References for MORB-OIB data bases and end-member mantle components are given in the caption of Fig. 1. Enlarged area focuses on the Antarctic data set.

PIMMS. The details of the analytical methods are described in the footnotes to Table 1. For several of the samples, Pb isotopes were measured on separate powder aliquots at both WHOI and ENSL and the data replicate well within analytical uncertainties (Table 1, Fig. 6). For three samples, Nd and Sr isotopes were independently measured by TIMS at UC Berkeley and the measurements replicate well within analytical uncertainties (Fig. 6). There is furthermore a good agreement with previously published Sr, Nd, and Pb isotopic data (Figs. 5 and 7; Sun and Hanson, 1975; Kyle et al., 1992). To our knowledge, these are the first measurements of Hf isotopes in Antarctic lavas.

The historic phonolite bombs exhibit limited variability in Sr, Nd, Hf, and Pb isotope compositions (Figs. 1–7; Tables 1 and 3), with the exception of the 1984 bombs, which have distinct Sr and Pb isotopic compositions. Excluding the 1984 bombs, the isotopic variability of the historic lava bombs is slightly larger than the internal measurement errors for individual samples. The variability of the historic bombs is essentially normally distributed and close to the reproducibility of the replicate measurements (Table 3). We therefore consider the isotopic compositions of the historic phonolite bombs to be uniform within analytical uncertainties, except for bombs erupted in 1984. The 1984 bombs have identical $^{143}Nd/^{144}Nd$ and $^{176}Hf/^{177}Hf$ to the other historic bombs, but their Pb isotopic compositions are less radiogenic and their $^{87}Sr/^{86}Sr$ are higher (Figs. 5 and 6). Although these differences are small, they are outside of the analytical uncertainty and have been replicated in different laboratories for three different 1984 bombs (Table 1).

The Sr, Nd, Hf, and Pb isotopic compositions of the 12 phase-three phonolite lavas from the summit area of Erebus are also essentially uniform and similar to the historic bombs (Figs. 1–7; Tables 1 and 3). The older basanites and phonotephrites are isotopically more variable and bracket the values observed for the younger lavas and bombs (Figs. 1–7; Tables 1 and 3). In these rocks the largest isotopic variation is observed for Pb and is dominated by the range in the DVDP lineage samples.

A tephriphonolite from Turks Head, which is part of the enriched Fe series, has the same $^{87}Sr/^{86}Sr$, ε_{Nd}, and ε_{Hf} as the EL phonolite lavas and bombs. The "Ice-Station" trachyte sample from the upper flanks of Mt. Erebus, which is the most differentiated end-member of the EFS, has a similar Nd isotopic composition, but distinctly lower $^{206}Pb/^{204}Pb$, $^{208}Pb/^{204}Pb$, and ε_{Hf} and higher $^{87}Sr/^{86}Sr$ compared to the EL phonolite lavas and bombs (Figs. 1–5 and 7; Table 1). These $^{87}Sr/^{86}Sr$ and Pb isotope values for the Ice-Station trachyte are similar to the $^{87}Sr/^{86}Sr$ values reported for the Aurora cliffs trachyte (83454) in Kyle et al. (1992) and the Pb isotope compositions reported for the Mt. Cis trachyte (13867) in Sun and Hanson (1975) (Figs. 5a and 7).

The three basanite samples from the adjacent Mt. Morning volcano are slightly offset from the Mt. Erebus lavas and bombs by having marginally higher $^{87}Sr/^{86}Sr$ and $^{208}Pb/^{204}Pb$, but lower $^{143}Nd/^{144}Nd$ and $^{206}Pb/^{204}Pb$ (Figs. 1–4; Table 1).

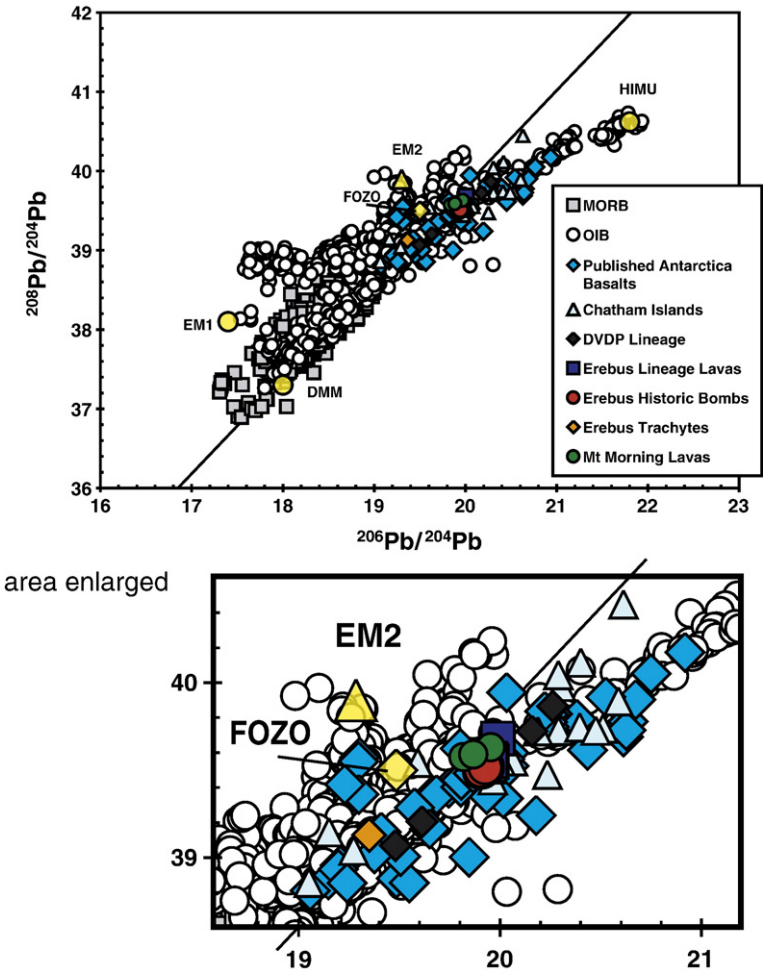

Fig. 3. $^{208}Pb/^{204}Pb$ versus $^{206}Pb/^{204}Pb$ for Erebus volcano, DVDP lineage, and Mt. Morning samples analyzed in this study. Also shown are the existing Pb isotope data from West Antarctic volcanics (Sun and Hanson, 1975; Hart et al., 1995, 1997; Panter et al., 2000) and the Chatham Islands (Panter et al., 2006). References for MORB-OIB data bases and end-member mantle components are given in the caption of Fig. 1. Enlarged area focuses on the Antarctic data set.

3.2. Pb isotopes in melt inclusions

Pb isotopes were measured in-situ on four glassy melt inclusions within an anorthoclase megacryst from a 1984 phonolitic bomb, and on four glassy melt inclusions within an olivine phenocryst from basanite DVDP 3-295. The in-situ measurements were conducted at WHOI using the Cameca IMS 1270 large format ion probe (Table 2 and Fig. 7) following procedures documented elsewhere (Saal et al., 1998). Because of the high concentrations of Pb in these melt inclusions, ion count rates were high enough to obtain reliable data not only for ^{208}Pb, ^{207}Pb, and ^{206}Pb, but also for ^{204}Pb. Analytical uncertainties ($^{206}Pb/^{204}Pb$ ~1.5%; $^{207}Pb/^{206}Pb$ ~0.6%; $^{208}Pb/^{206}Pb$ ~0.5%; 1σ) nevertheless are much higher than with PIMMS (~100–200 ppm) or TIMS (~2–5 per mil) but within error the in-situ Pb isotope measurements agree with the PIMMS and TIMS data for the phenocryst host lavas (Fig. 7).

4. Discussion

4.1. Characterization of the Erebus mantle source

All of the Erebus volcano and DVDP samples, except for the trachyte, have radiogenic $^{206}Pb/^{204}Pb$ and $^{208}Pb/^{204}Pb$, unradiogenic $^{87}Sr/^{86}Sr$, and intermediate $^{143}Nd/^{144}Nd$ and $^{176}Hf/^{177}Hf$ (Figs. 1–3). They lie along a trajectory between DMM, as defined by MORB, and the HIMU end-member mantle component, as defined by samples from Mangaia-Tubuai. They also lie between HIMU and the theoretical mantle component 'FOZO' as defined by Hart et al. (1992).

Several studies have shown that the 'HIMU' signature is a seemingly ubiquitous characteristic of Antarctica, the sub-Antarctic islands, and some New Zealand Cenozoic volcanism (Sun and Hanson, 1975; Rocholl et al., 1995; Hart et al., 1995, 1997; Panter et al., 2000; Finn et al., 2005; Panter et al., 2006). However, there is little agreement on the genesis and pedigree of the HIMU source component beneath Antarctica (Kyle et al., 1992; Hart et al., 1995, 1997; Worner, 1999; Finn et al., 2005; Panter et al., 2006). Noting the large volume of magma erupted over a short period of time (~4,520 km^3 over the last ~4 Ma; Esser et al., 2004) and that the isotopic (Figs. 1–4) and trace element characteristics of MVG lavas are similar to other 'HIMU' OIB (Fig. 8), Sun and Hanson (1975) and Kyle et al. (1992) suggested that Ross Island in general, and Erebus volcano in particular, is the manifestation of an upwelling mantle plume or a hot spot. Recent travel time tomography indicating a deep thermal anomaly beneath Ross Island (Watson et al., 2006) is consistent with this hypothesis. However, the wide regional scope of the 'HIMU signature' in West Antarctic volcanoes (Figs. 1, 3 and 4) has been difficult to reconcile with a simple plume hypothesis, leading other more recent studies to suggest that the source of Antarctic Cenozoic basaltic volcanism is not upwelling asthenospheric mantle, but rather thick lithospheric mantle impregnated with amphibole and phlogopite veins (Panter et al., 2006). In this scenario, the HIMU isotopic signature is an in-grown feature of the lithosphere, generated by partial dehydration

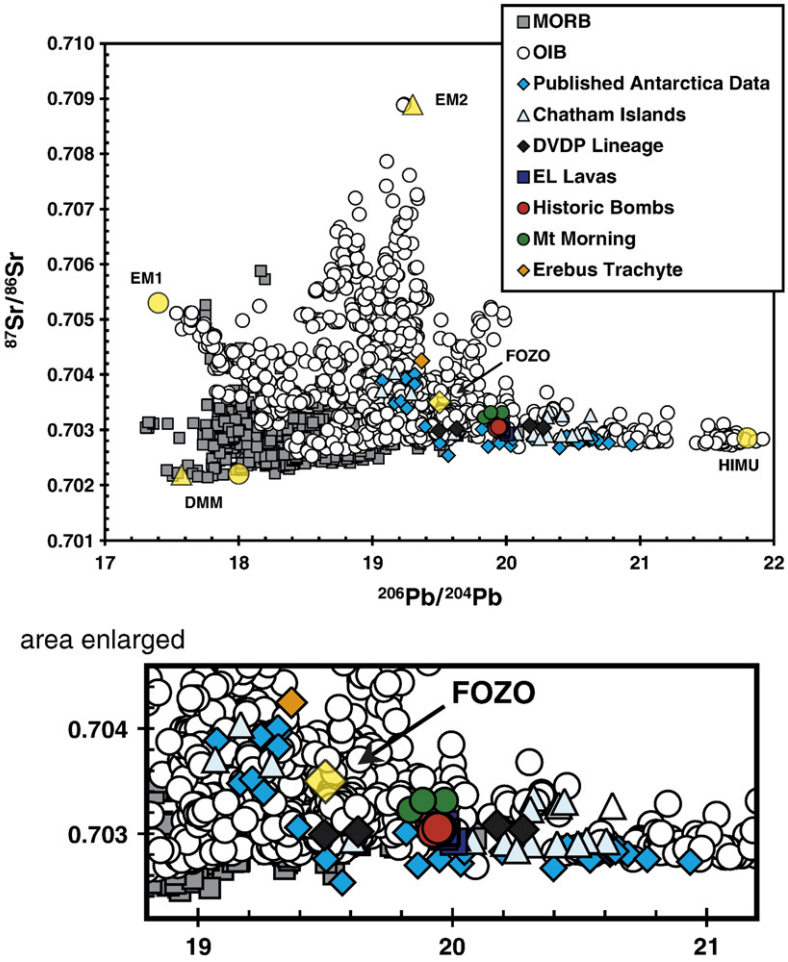

Fig. 4. $^{87}Sr/^{86}Sr$ versus $^{206}Pb/^{204}Pb$ for Erebus volcano, DVDP lineage, and Mt. Morning samples analyzed in this study. Also shown are the existing Sr and Pb isotope data from West Antarctic volcanics (Sun and Hanson, 1975; Hart et al., 1995, 1997; Panter et al., 2000) and the Chatham Islands (Panter et al., 2006). References for MORB-OIB data bases and end-member mantle components are given in the caption of Fig. 1. Enlarged area focuses on the Antarctic data set.

and loss of hydrophile elements (Pb, Rb, K) relative to the more magmaphile elements (Th, U, Sr) during plume- and/or subduction-related metasomatism taking place somewhere between 100–500 My ago.

The Erebus samples show an extremely limited range of Sr, Nd, Hf, and Pb isotopic compositions, which are most straightforwardly accounted for by simple two-component mixing of the mantle end-member components DMM and HIMU. Most other Antarctic and New Zealand volcanic suites show substantially larger isotopic variability (see Figs. 1–4), with some (e.g. Peter 1, Jones Island, Chatham Islands, and Mt. Morning) even requiring an additional enriched mantle component(s) to account for their combined Nd, Sr, and Pb isotopic signatures (Hart et al., 1995, 1997; Finn et al., 2005, Panter et al., 2006). The Erebus trachytes are distinct from the other enriched Antarctic lava samples in that they have higher $^{87}Sr/^{86}Sr$ and lower $^{206}Pb/^{204}Pb$ and $^{208}Pb/^{204}Pb$. As will be discussed in detail below, these trachyte lavas are unique from the rest of the Erebus lineage in that they appear to have assimilated continental crust during their petrogenesis and subsequent evolution.

While our new Nd, Sr, Hf, and Pb isotopic data do not unambiguously distinguish between whether the Erebus volcano HIMU signature results from melting of an upwelling asthenospheric mantle plume or rather reflects vein-infused lithospheric mantle, it is important to note that all four isotopic systems are best explained by simple two-component mixing of DMM and HIMU. This suggests that the Erebus HIMU signature is not due to lithospheric enrichment produced within the last 100–500 Ma, but rather is a more ancient source component, with long-term U/Pb, Sm/Nd, Rb/Sr, and Lu/Hf characteristics similar to the HIMU end-member source defined by Mangaia-Tubuai. This time constraint (>500 Ma) is particularly important for the ^{147}Sm–^{143}Nd isotope system for which the long half-life of ^{147}Sm of 106 Ga implies that the $^{143}Nd/^{144}Nd$ of a recently vein-infused lithospheric mantle would not change much over 100–500 Ma.

4.2. Temporal variations in Sr, Nd, Hf, and Pb isotopes

In principle, geochemical time series can constrain the dynamics of magmatic processes (Reagan et al., 1987; Albarède, 1993; Francalanci et al., 1999; Hawkesworth et al., 2000, 2004) and even potentially aid in forecasting major eruptions (Chen et al., 1993). The persistent and well-sampled Strombolian activity of Erebus volcano (Kyle et al., 1992; Caldwell and Kyle, 1994; Kelly et al., 2007-this volume-a) coupled with its well-dated lava sequence provide a unique opportunity to study the temporal evolution of this alkaline volcano.

We note four distinct features (Figs. 5 and 6) in the Erebus time series data:

1) The isotopic compositions of the early EL and DVDP lineage lavas are more variable than the historic phonolite bombs, particularly for Pb isotopes. These older DVDP and EL lavas are less evolved (basanite to phonotephrite) and derive from small isolated volcanic

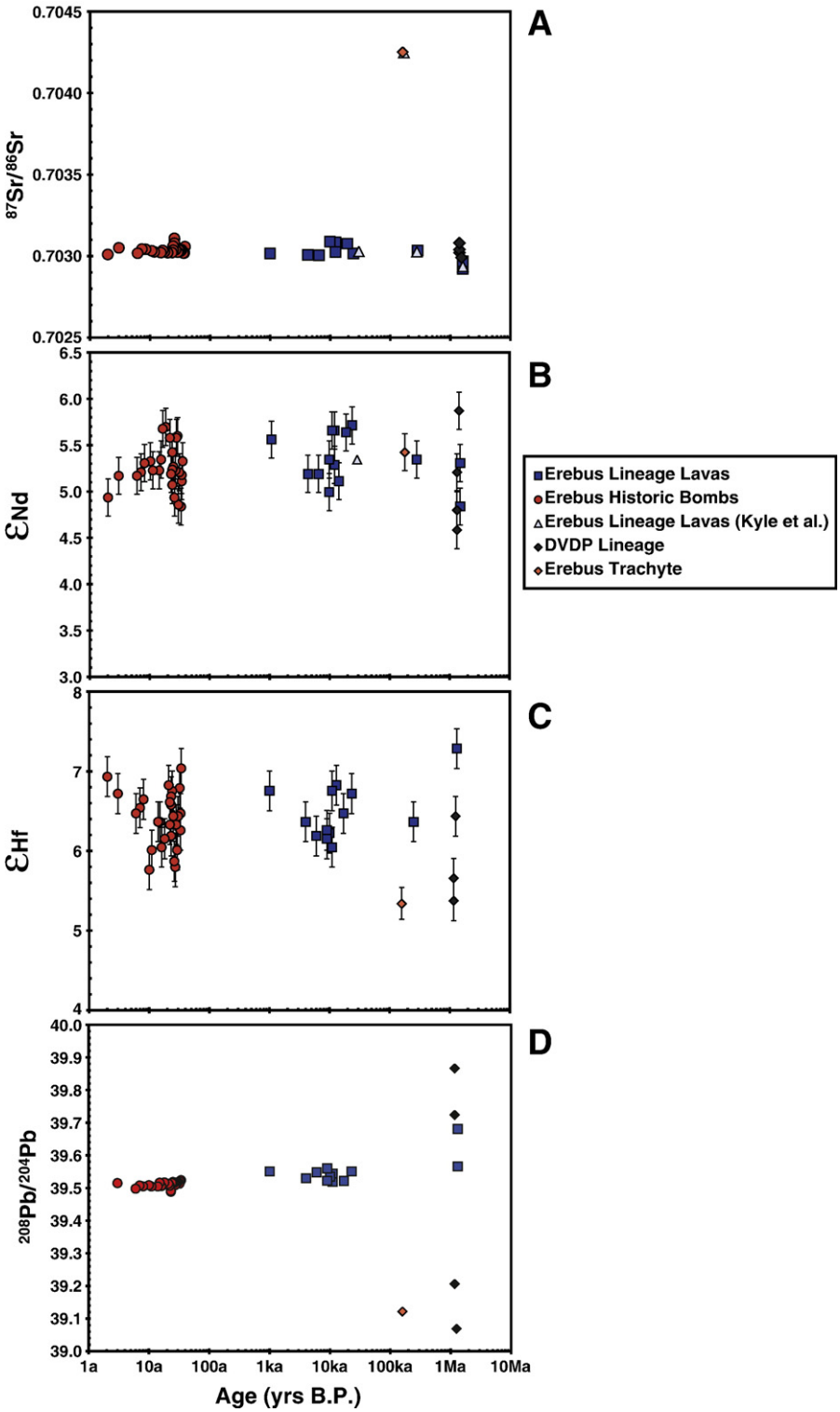

Fig. 5. A) $^{87}Sr/^{86}Sr$, B) ε_{Nd}, C) ε_{Hf}, and D) $^{206}Pb/^{204}Pb$ versus time for Erebus volcano and DVDP lineage samples. Also shown are the ε_{Nd} (1 sample) and $^{87}Sr/^{86}Sr$ (4 samples) data from Kyle et al. (1992).

centers surrounding Mt. Erebus. Hence, during the early development of the Erebus edifice and the DVDP lavas, isotopically disparate batches of melts, resulting from small degrees of melting, erupted with minimal interaction and mixing.

2) Sr, Nd, Hf, and Pb isotopes for the younger phonolitic lavas and recent bombs are essentially invariant over the past ~17 ka. Except for the effects of different modal abundances of anorthoclase, the major and trace element compositions of these samples also are uniform (Kyle et al., 1992; Caldwell and Kyle, 1994; Kelly et al., 2007-this volume-a). The relative compositional uniformity of these samples suggests that the Erebus magmatic system currently is stable (i.e., in a steady-state) and that either its source is isotopically homogeneous, or mixing of batches of parental basanite with different isotopic compositions is extremely efficient.

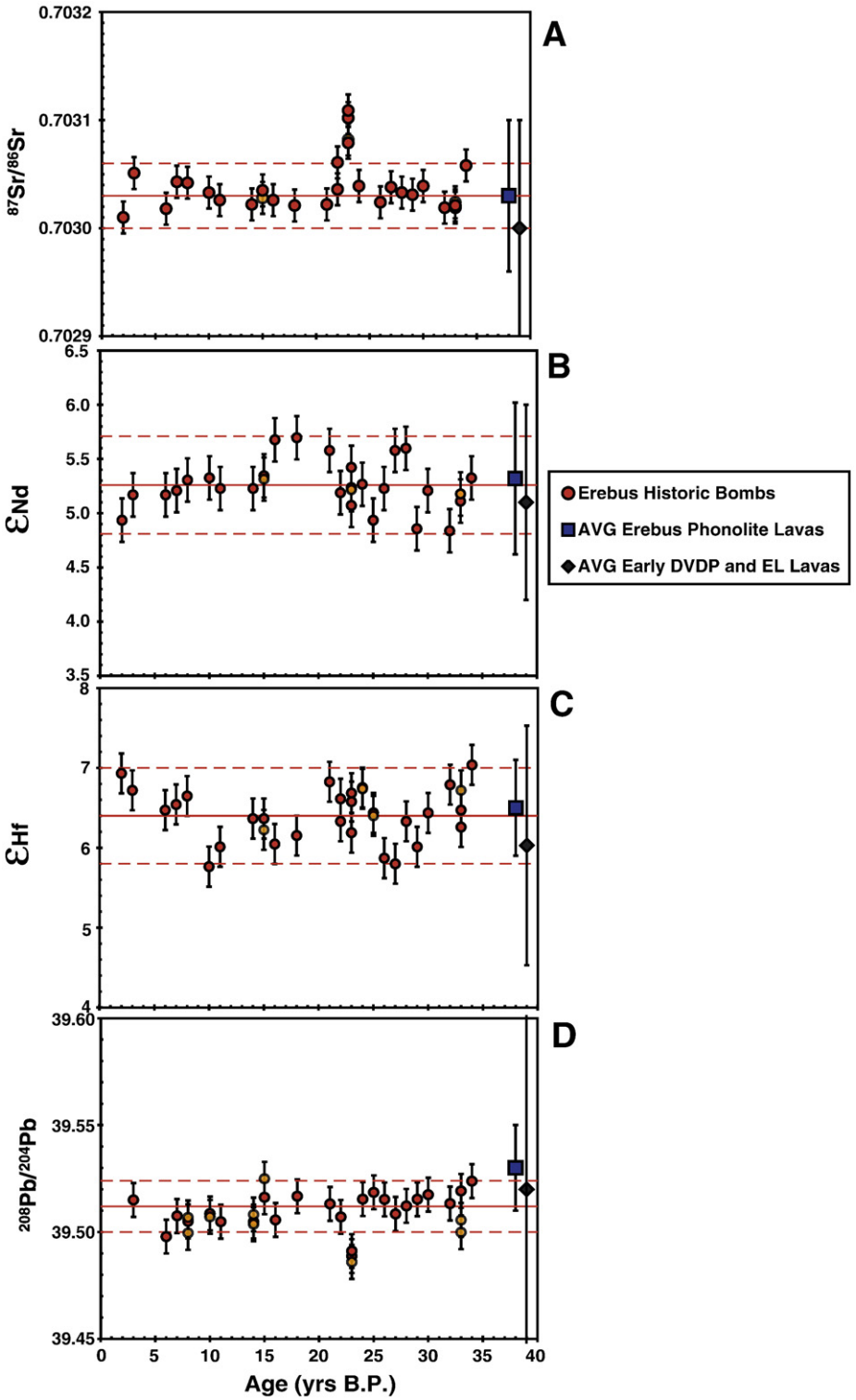

Fig. 6. A) $^{87}Sr/^{86}Sr$, B) ε_{Nd}, C) ε_{Hf}, and D) $^{206}Pb/^{204}Pb$ versus time for Erebus historic phonolites erupted from Erebus volcano. Sample replicates are shown in a lighter shade of red/orange. Averages (solid red line) and two-sigma standard deviations on the mean (dashed red lines) for these samples are indicated. Also shown are the averages and two-sigma standard deviations for the dated Erebus phonolite lavas (blue squares) and phase-one and -two Erebus and DVDP lineage basanites, phonotephrites, and tephriphonolites.

Both the EL and DVDP lineage lavas range from basanite to phonolite and show a distinct "step function" in isotopic variability as a function of the extent of differentiation. The average $^{143}Nd/^{144}Nd$, $^{87}Sr/^{86}Sr$, $^{176}Hf/^{177}Hf$, $^{206}Pb/^{204}Pb$, $^{207}Pb/^{204}Pb$, and $^{208}Pb/^{204}Pb$ of the basanites is similar to the averages of the phonolite lavas and bombs (Table 3; Figs. 5 and 6). We interpret these observations as an indication that magma mixing of the primary basanites during magma generation and storage, and prior to differentiation, has played a fundamental role in establishing the isotopic and compositional uniformity of these differentiated samples. This conclusion differs from Kyle et al. (1992), who, based on a limited set of Sr isotope data, concluded that the EL represents simple fractional

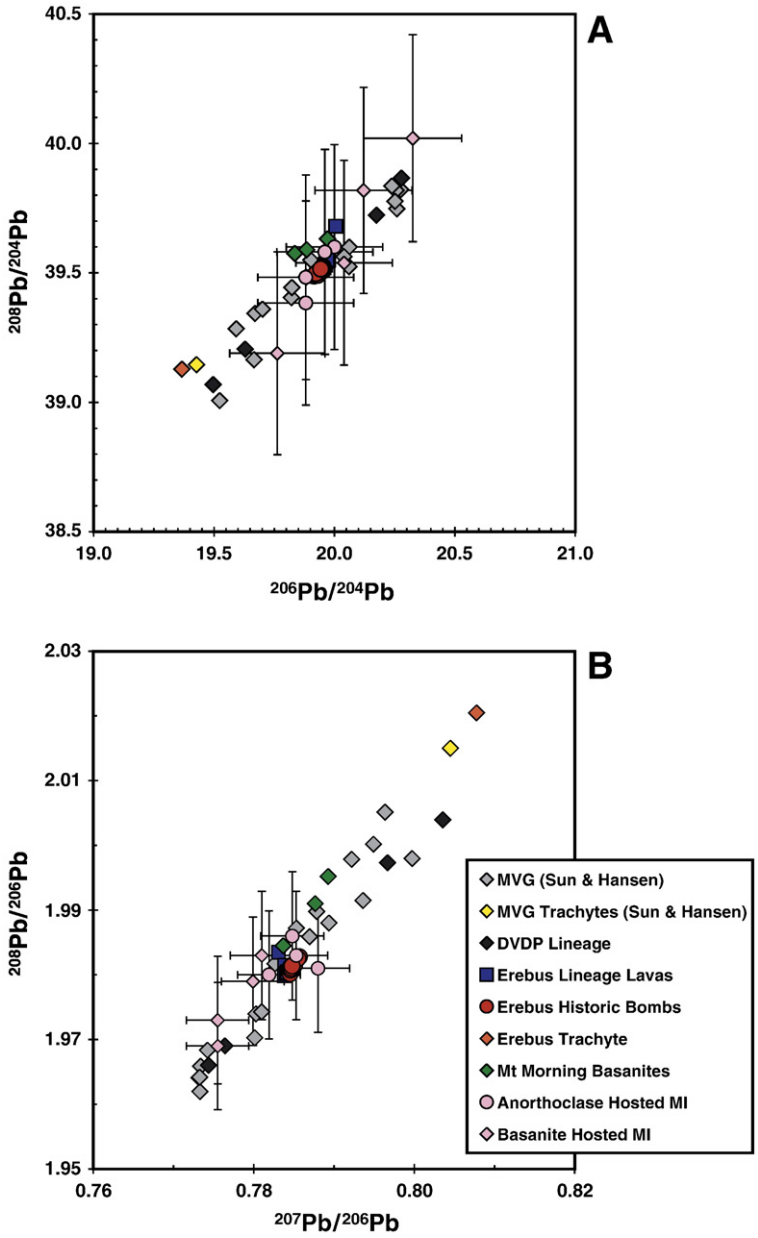

Fig. 7. A) $^{208}Pb/^{204}Pb$ versus $^{206}Pb/^{204}Pb$ and B) $^{208}Pb/^{206}Pb$ versus $^{207}Pb/^{206}Pb$ for Erebus volcano, DVDP lineage, and Mt Morning samples analyzed by PIMMS and anorthoclase megacryst and olivine-hosted melt inclusions analyzed by SIMS. Also shown are the existing Pb isotope data for McMurdo Volcanics measured by TIMS by Sun and Hanson (1975).

crystallization of compositionally uniform melts coming from a homogeneous mantle source. Clearly, the Pb isotopic data for the basanites demonstrate that the mantle source is variable, but this is difficult to reconcile with the uniformity of the differentiates at Erebus volcano. Mixing of the parental basanites in a large magma chamber thus seems to be the best way to account for the isotopic composition of the Erebus lavas.

3) The trachyte sample from the EFS has elevated $^{87}Sr/^{86}Sr$ and low $^{206}Pb/^{204}Pb$ and $^{208}Pb/^{204}Pb$ (Table 1; Figs. 5 and 7). These distinct Sr and Pb isotope signatures confirm earlier measurements (Sun and Hanson, 1975; Kyle et al., 1992) and support the hypothesis that the Fe-enriched trachytes have assimilated continental crust during their genesis (Kyle et al., 1992). This is in marked contrast to the evolution of the phonolitic lavas, which are related to the parental basanites along a single liquid-line of descent without any discernable crustal assimilation.
4) The 1984 bombs have the same $^{143}Nd/^{144}Nd$ and $^{176}Hf/^{177}Hf$ as the other historic bombs, whereas their $^{206}Pb/^{204}Pb$ and $^{208}Pb/^{204}Pb$ are lower and their $^{87}Sr/^{86}Sr$ higher (Figs. 5 and 6; Table 1). Although these differences admittedly are small, they are outside of the 1984 bombs' analytical uncertainty and the standard deviation of the 'historic bomb average', and are thus possibly real. The ($^{238}U/^{232}Th$), ($^{230}Th/^{232}Th$), and ($^{230}Th/^{238}U$) obtained on 1984 bombs are also slightly different from the rest of the historic bomb suite (Sims et al., 2007-this volume). In terms of historical eruptive activity, 1984 was an exceptional year with larger and more frequent Strombolian eruptions (Kyle, 1986; Caldwell and Kyle, 1994) than previous and following years. If this increased activity reflects additional magma input or changes in the conduit system, then very minor assimilation can be invoked to explain the observed Sr and Pb isotopic shifts. The isotopic shift in Sr and Pb isotopes of the 1984 bombs is in the direction of the 170 ka trachytes. The trace element compositions of these trachytes are similar to those of the phonolite lavas and bombs (Fig. 8), except for Sr and Pb, whose concentrations are affected by removal or addition of anorthoclase. Mass balance calculations show that admixing less than 3% average

Table 2
Pb isotopes from glassy melt inclusions in an anorthoclase megacryst from a 1984 Erebus bomb, and in olivine from DVDP-3

Sample	$^{204}Pb/^{206}Pb$	$^{207}Pb/^{206}Pb$	$^{208}Pb/^{206}Pb$	Intensity ^{208}Pb (CPS)
Anorthoclase hosted melt inclusions from 1984 bomb				
AM1 (rim)	0.0500	0.7819	1.980	356
AM2	0.0501	0.7853	1.983	307
AM3	0.0503	0.7880	1.981	308
AM4 (center)	0.0503	0.7848	1.986	365
DVDP 3 olivine hosted melt inclusions				
OM1	0.0506	0.7810	1.983	278
OM2	0.0497	0.7799	1.979	368
OM3	0.0492	0.7755	1.969	443
OM4	0.0499	0.7755	1.973	310

One-sigma uncertainties based on in-run analytical errors are 1–5% for $^{204}Pb/^{206}Pb$, 0.4–0.7% for $^{207}Pb/^{206}Pb$, and 0.4–0.6% for $^{208}Pb/^{206}Pb$. Intensity of ^{208}Pb signal is given as counts per second (CPS).

trachyte with average phonolite bomb glass changes the Sr and Pb isotope compositions by the required amount without significantly affecting the major and trace element abundances of the phonolitic lavas (i.e., when taking into account the analytical uncertainties on the trace element data), which would account for the uniformity of trace element abundances among the Erebus bombs, including those of 1984 (for major and trace element abundances see Kelly et al., 2007-this volume-a). Assimilation of Erebus phonolite is also likely to occur during conduit adjustments/changes, but this will not manifest itself in Nd, Sr, Pb, or Hf isotopic changes unless the rock is secondarily altered and its isotopic composition perturbed.

4.3. Pb isotopes in melt inclusions

In principle, in-situ measurements of Pb isotopes in melt inclusions provide information on the isotopic composition of the magma in which the crystal grew. In many previous studies, the range of the isotopic compositions of melt inclusions exceeds, often by far, the variation in the volcanic suite from which the lava was collected (Saal et al., 1998) and is thus interpreted as reflecting isotopic heterogeneity in the pre-aggregated melt.

The Pb isotope compositions of the melt inclusions from the 1984 anorthoclase megacryst are uniform and, within analytical uncertainties, similar to those of the host lava (Fig. 7). This isotopic homogeneity among the melt inclusions suggests that the phonolite magma was well mixed at the time of its incorporation into the anorthoclase crystal, which is not surprising given that these melt inclusions are highly degassed (H_2O — 0.17±0.02 wt.%; CO_2 — 690±125 ppm; S — 375±60 ppm) and thus interpreted to have been growing at shallow levels in the Erebus conduit (Dunbar et al., 1994; Eschenbacher et al., 2007-this volume).

Again within analytical uncertainties, the Pb isotopic compositions of the melt inclusions in the basanite olivine are also homogeneous and show slightly less variability than observed for the DVDP lavas (Fig. 7). Contrary to the melt inclusions of the anorthoclase megacryst, the olivine-hosted melt inclusions have high volatile contents (H_2O ~ 1–1.5 wt.%; CO_2 ~ 4000–7300 ppm; S ~ 2500 ppm) and are interpreted to have grown at much deeper levels (~3 to 4 kbars) in the magmatic system (Eschenbacher et al., 2007-this volume). The large analytical uncertainties associated with the melt inclusion measurements, however, limit the present interpretation of the data to simply suggesting that the basanitic magma was already well mixed at the time of its incorporation into the olivine.

5. Conclusions

1) All of the Erebus volcano and DVDP samples, except for the trachyte, have radiogenic $^{206}Pb/^{204}Pb$ and $^{208}Pb/^{204}Pb$, unradiogenic $^{87}Sr/^{86}Sr$, and intermediate $^{143}Nd/^{144}Nd$ and $^{176}Hf/^{177}Hf$, and lie along a mixing trajectory between the end-member mantle components DMM, as defined by MORB, and HIMU, as defined by Mangaia-Tubuai.
2) There is a marked distinction between the older EL and DVDP basanites and phonotephrites, whose Nd, Sr, Hf, and Pb isotopes are variable (particularly Pb), and the younger phonolitic lavas and bombs, whose Nd, Sr, Hf, and Pb isotopes are essentially invariant. Taken together, these Erebus and DVDP samples define a step function in which isotopic variability decreases with extent of differentiation indicating that mixing of the parental basanites has played a fundamental role in establishing the isotopic and compositional uniformity of the younger phonolites.

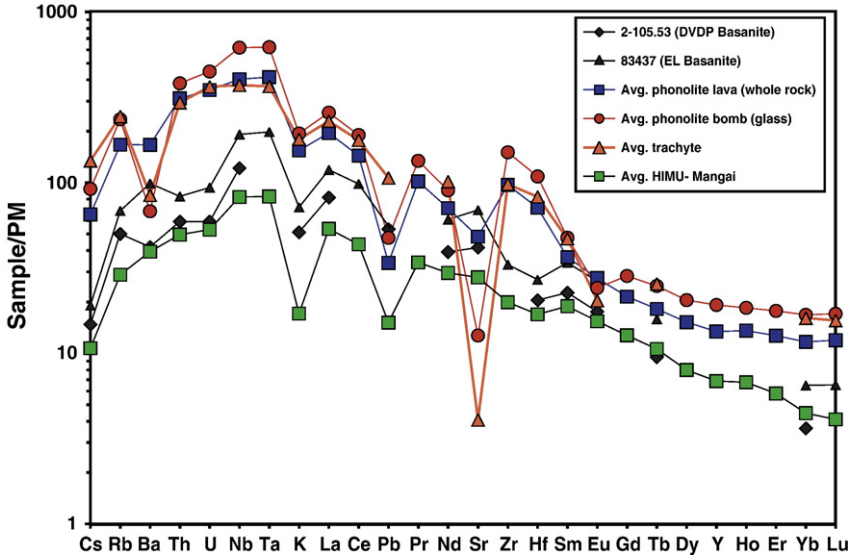

Fig. 8. PUM-normalized trace element plots for DVDP basanites and Mt. Erebus dated phonolitic lavas and recently erupted bombs and dated trachyte lavas. Normalized to primitive mantle (pyrolite) values from McDonough and Sun (1995).

Table 3
Mean, standard deviation, median, kurtosis, and skewness of the distribution and range of EL and DVDP lineage lavas

	$^{206}Pb/^{204}Pb$	$^{207}Pb/^{204}Pb$	$^{208}Pb/^{204}Pb$	$^{87}Sr/^{86}Sr$	$^{143}Nd/^{144}Nd$	$^{176}Hf/^{177}Hf$
Historic phonolite bombs						
Including 1984 bombs						
N	25	25	25	27	26	28
Mean	19.941	15.649	39.509	0.70304	0.51291	0.28295
S.D. (2σ)	0.019	0.004	0.018	0.00005	0.00002	0.00002
Median	19.944	15.649	39.512	0.70303	0.51291	0.28295
Skewness	−1.47	0.64	−0.86	1.85	0.18	−0.17
Kurtosis	1.60	1.03	0.20	3.49	−0.28	−0.64
Min.	19.916	15.646	39.489	0.70301	0.51289	0.28294
Max.	19.953	15.653	39.524	0.70312	0.51293	0.28297
Excluding 1984 bombs						
N	22	22	22	24	24	25
Mean	19.944	15.649	39.512	0.70303	0.51291	0.28295
S.D. (2σ)	0.012	0.004	0.012	0.00003	0.00002	0.00002
Median	19.945	15.649	39.513	0.70303	0.51291	0.282952
Skewness	−1.70	0.45	−0.30	0.64	0.19	−0.10
Kurtosis	5.06	1.04	−0.25	0.00	−0.26	−0.70
Min.	19.923	15.646	39.498	0.70301	0.51289	0.28294
Max.	19.953	15.653	39.524	0.70306	0.51293	0.28297
EL phonolite lavas						
N	11	11	11	9	12	12
Mean	19.965	15.655	39.537	0.703046	0.512911	0.282955
S.D. (2σ)	0.014	0.010	0.025	0.000075	0.000035	0.000017
Median	19.963	15.654	39.535	0.703025	0.512911	0.282954
Skewness	0.27	0.30	−0.10	0.21	−0.85	0.04
Kurtosis	−1.19	−1.43	−1.80	−2.39	0.60	−1.86
Min.	19.957	15.649	39.519	0.70301	0.51287	0.28294
Max.	19.976	15.663	39.552	0.70309	0.51293	0.28297
Stage 1 EL and DVDP lavas						
N	6	6	6	6	6	5
Mean	19.925	15.664	39.519	0.70300	0.51290	0.28294
S.D. (2σ)	0.611	0.043	0.627	0.00011	0.00005	0.00005
Median	19.987	15.665	39.623	0.70301	0.51290	0.28293
Skewness	−0.47	0.99	−0.65	−0.15	0.85	1.08
Kurtosis	−1.35	2.16	−1.36	−0.26	0.40	−0.20
Min.	19.496	15.638	39.069	0.70292	0.51287	0.28292
Max.	20.278	15.702	39.866	0.70308	0.51294	0.28298

3) A trachyte sample from the enriched Fe series has elevated $^{87}Sr/^{86}Sr$ and low $^{206}Pb/^{204}Pb$ supporting the hypothesis that the Fe-enriched trachytes have assimilated continental crust during their genesis (Kyle et al., 1992).
4) For the 1984 bombs, $^{143}Nd/^{144}Nd$ and $^{176}Hf/^{177}Hf$ are the same as for the other historic bombs, but their $^{206}Pb/^{204}Pb$ is lower and their $^{87}Sr/^{86}Sr$ higher (Figs. 5 and 6). These differences are small, but significant, and can be interpreted in terms of assimilation of Erebus trachyte.
5) The Pb isotopic compositions of the melt inclusions from both the 1984 anorthoclase megacryst and the basanitic olivine are uniform and the same as the host lavas, within analytical uncertainties (Fig. 7). While the large uncertainties associated with these melt inclusion measurements limit the interpretation of the data, the striking isotopic homogeneity nevertheless suggests, in both cases, that the magma was well mixed at the time of its incorporation into these different phases. This result is not surprising for the melt inclusions from the anorthoclase crystals, as these crystallized in a shallow, steady-state, differentiated magma system, but was not necessarily expected for the basanitic olivine-hosted melt inclusions, which formed much deeper in the system.

Acknowledgments

This work was supported by the Office of Polar Program, NSF grant OPP-0126269 to Ken Sims and grants OPP-0125744, OPP-0229305, ANT-0538414 to Philip Kyle. Janne Blichert-Toft acknowledges financial support from the French Institut National des Sciences de l'Univers. Reviews and comments by Stan Hart, Kurt Panter, Andreas Stracke, and an anonymous reviewer are appreciatively acknowledged.

References

Agranier, A., Blichert-Toft, J., Graham, D., Debaille, V., Schiano, P., Albarede, F., 2005. The spectra of isotopic heterogeneity along the mid-Atlantic Ridge. Earth Planet. Sci. Lett. 238, 96–109.
Albarède, F., 1993. Residence time analysis of geochemical fluctuations in volcanic series. Geochim. Cosmochim. Acta 57, 615–621.
Bannister, S., Snieder, R.K., Passier, M.L., 2000. Shear-wave velocities under the Transantarctic Mountains and Terror Rift from surface wave inversion. Geophys. Res. Lett. 27, 281–284.
Behrendt, J.C., 1999. Crustal and lithospheric structure of the West Antarctic Rift System from geophysical investigations — a review. Glob. Planet. Change 23, 25–44.
Behrendt, J.C., LeMasurier, W.E., Cooper, A.K., Tessensohn, F., Trehu, A., Damaske, D., 1991. Geophysical studies of the West Antarctic rift system. Tectonics 10, 1257–1273.
Blichert-Toft, J., Albarède, F., 1997. The Lu-Hf isotope geochemistry of chondrites and the evolution of the mantle-crust system. Earth Planet. Sci. Lett. 148, 243–258.
Blichert-Toft, J., Chauvel, C., Albarède, F., 1997. Separation of Hf and Lu for high-precision isotope analysis of rock samples by magnetic sector-multiple collector ICP-MS. Contrib. Mineral. Petrol. 127, 248–260.
Caldwell, D., Kyle, P.R., 1994. Mineralogy and geochemistry of ejecta erupted from Mount Erebus, Antarctica between 1972 and 1986. In: Kyle, P.R. (Ed.), Volcanological and Environmental Studies of Mount Erebus, Antarctica. . Antarct. Res. Ser., vol. 66. Am Geophys Union, Washington, D.C., pp. 147–162.
Chen, C.H., DePaolo, D.J., Nakada, S., Shieh, Y.N., 1993. Relationship between eruption volume and neodymium isotopic composition at Unzen volcano. Nature 362, 831–834.
Cooper, A.K., Davey, F.J., Behrendt, J.C., 1987. Seismic stratigraphy and structure of the Victoria Land basin, western Ross Sea, Antarctica. In: Cooper, A.K., Davey, F.J. (Eds.), The Antarctic Continental Margin: geology and geophysics of the western Ross Sea. Circum-Pacific Council for Energy and Resources, Houston, pp. 27–65.

Dunbar, N., Cashman, K., Dupre, R., 1994. Crystallization processes of anorthoclase phenocrysts in the Mount Erebus magmatic system: evidence from crystal composition, crystal size distributions and volatile contents of melt inclusions. In: Kyle, P.R. (Ed.), Volcanological and Environmental Studies of Mount Erebus, Antarctica. Antarct. Res. Ser., vol. 66. AGU, Washington, D.C., pp. 129–146.

Eschenbacher, A., Kyle, P.R., Lowernstern, J., Hervig, R., Oppenheimer, C., Dunbar, N.W., 2007-this volume. Pre-eruptive Volatile Contents of Alkalic Magmas, Erebus Volcano, Antarctica.

Esser, R.P., Kyle, P.R., McIntosh, W.C., 2004. $^{40}Ar/^{39}Ar$ dating of the eruptive history of Mount Erebus, Antarctica: volcano evolution. Bull. Volcanol. 66, 671–686.

Finn, C.A., Müller, R.D., Panter, K.S., 2005. A Cenozoic diffuse alkaline magmatic province (DAMP) in the southwest Pacific without rift or plume origin. Geochem. Geophys. Geosyst. 6, Q02005, doi:10.1029/2004GC000723.

Francalanci, L., Tommasini, S., Conticelli, S., Davies, G.R., 1999. Sr isotope evidence for short magma residence time for the 20th century activity at Stromboli volcano, Italy. Earth Planet. Sci. Lett. 167, 61–69.

Futa, K., LeMasurier, W.E., 1983. Nd and Sr isotopic studies on Cenozoic mafic lavas from West Antarctica: another source for continental alkali basalts. Contrib. Mineral. Petrol. 83, 38–44.

Giggenbach, W., Kyle, P., Lyon, G., 1973. Present volcanic activity on Mt. Erebus, Ross Island, Antarctica. Geology 1, 135–156.

Harpel, C.J., Kyle, P.R., Caldwell, D.A., McIntosh, W.C., Esser, R.P., 2004. $^{40}Ar/^{39}Ar$ dating of the eruptive history of Mount Erebus, Antarctica: summit flows and caldera collapse. Bull. Volcanol. 66, 687–702.

Harpel, C.J., Kyle, P.R , Dunbar, N.W., 2007-this volume. Englacial tephrostratigraphy of Mount Erebus volcano, Antarctica. Journ. Vol. Geotherm Res.

Hart, S.R., Blusztajn, J., 2006. Age and geochemistry of the mafic sills, ODP site 1276, New Foundland margin. Chem. Geol, doi:10.1016/j.chemgeo.2006.07.001.

Hart, S.R., Hauri, E.H., Oschmann, L.A., Whitehead, J.A., 1992. Mantle plumes and entrainment-isotopic evidence. Science 256, 517–520.

Hart, S.R., Blusztajn, J., Craddock, C., 1995. Cenozoic volcanism in Antarctica; Jones Mountains and Peter I Island. Geochim. Cosmochim. Acta 59, 3379–3388.

Hart, S.R., Blusztajn, J., LeMasurier, W.E., Rex, D.C., 1997. Hobbs Coast Cenozoic volcanism: implications for the West Antarctic rift system. Chem. Geol. 139, 223–248.

Hart, S.R., Workman, R.K., Ball, L., Blusztajn, J., 2004. High precision Pb isotope techniques from the WHOI NEPTUNE PIMMS. WHOI Plasma Facility Open File Technical Report, vol. 10. http://www.whoi.edu/science/GG/people/shart/open_file.htm.

Hart, S.R., Ball, L., Jackson, M., 2005. Sr isotopes by laser ablation PIMMS: application to CPX from Samoan peridotite xenoliths. WHOI Plasma Facility Open File Technical Report, vol. 11. http://www.whoi.edu/science/GG/people/shart/open_file.htm.

Hawkesworth, C., Blake, S., Evans, P., Hughes, R., MacDonald, R., Thomas, L.E., Turner, S.P., Zellmer, G., 2000. Time scales of crystal fractionation in magma chambers — integrating physical, isotopic and geochemical perspectives. J. Petrol. 41, 991–1006.

Hawkesworth, C., Rhiannon, G., Turner, S., Zellmer, G., 2004. Time scales of magmatic processes. Earth Planet. Sci. Lett. 218, 1–16.

Kyle, P.R., 1981. Mineralogy and geochemistry of a basanite to phonolite lava sequence at Hut Point Peninsula, Antarctica, based on core from Dry Valley Drilling Project Holes 1, 2 and 3. J. Petrol. 22 (4), 451–500.

Kyle, P., 1986. Volcanic activity of Mount Erebus, 1984–1986. Antarct. J. U.S. XXI, 7–8.

Kyle, P.R., 1990a. McMurdo Volcanic Group Western Ross Embayment: introduction. In: LeMasurier, W., Thompson, J. (Eds.), Volcanoes of the Antarctic Plate and Southern Oceans. Ant. Res. Series, vol. 48. American Geophysical Union, pp. 18–25.

Kyle, P.R., 1990b. Erebus volcanic Province: summary. In: LeMasurier, W., Thompson, J. (Eds.), Volcanoes of the Antarctic Plate and Southern Oceans. . Antarctic Research Series, vol. 48. American Geophysical Union, pp. 81–88.

Kyle, P., Dibble, R., Giggenbach, W., Keys, J., 1982. Volcanic activity associated with the anorthoclase phonolite lava lake, Mt. Erebus, Antarctica. In: Craddock, C. (Ed.), Antarctic Geosciences. Univ. Wisc. Press, Madison, pp. 735–745.

Kyle, P.R., Moore, J.A., Thirlwall, M.F., 1992. Petrologic evolution of anorthoclase phonolite lavas at Mount Erebus, Ross Island, Antarctica. J. Petrol. 33, 849–875.

Kelly, P.J., Kyle, P.R., Dunbar N.W., Sims K.W.W. 2007-this volume-a. Geochemistry and mineralogy of the phonolite lava lake, Mount Erebus volcano, Antarctica: 1972–2004 and comparison with older lavas. Journ. Vol. Geotherm Res.

Kelly, P., Dunbar, N., Kyle, P.R., McIntosh, W.C. 2007-this volume-b. Refinement of the younger geologic history of Erebus volcano, Antarctica using $^{40}Ar/^{39}Ar$ and ^{36}Cl age determinations. Journ. Vol. Geotherm Res.

LeBas, M.J., LeMaitre, R.W., Streckeisen, A., Zanettin, B., 1986. A chemical classification of volcanic rocks based on the total alkali silica diagram. J. Petrol. 27, 745–750.

McDonough, W.F., Sun, S.-S., 1995. The composition of the Earth. Chem. Geol. 120, 223–253.

Moore, J.A., Kyle, P.R., 1987. Volcanic geology of Mt. Erebus, Ross Island, Antarctica. Proceedings of NIPR Symposium on Antarctic Geoscience, vol. 1, pp. 46–65.

Moore, J.A., Kyle, P.R., 1990. A.17. Mount Erebus. In: LeMasurier, W., Thompson, J. (Eds.), Volcanoes of the Antarctic Plate and Southern Oceans. Ant. Res. Series, vol. 48. American Geophysical Union, pp. 103–108.

Oppenheir, C., Kyle, P.R., 2007-this volume. Probing the magma plumbing of Erebus volcano, Antarctica, by open-path FTIR spectroscopy of gas emissions. Journ. Vol. Geotherm Res.

Panter, K.S., Hart, S.R., Kyle, P., Blusztanjn, J., Wilch, T., 2000. Geochemistry of Late Cenozoic basalts from the Crary Mountains: characterization of mantle sources in Marie Byrd Land, Antarctica. Chem. Geol. 165, 215–241.

Panter, K.S., Blusztajn, J., Hart, S.R., Kyle, P.R., Esser, R., McIntosh, W.C., 2006. The Origin of HIMU in the SW Pacific: evidence from intraplate volcanism in southern New Zealand and Subantarctic Islands. J. Petrol. 47, 1673–1704.

Reagan, M., Gill, J., Malavassi, E., Garcia, M.O., 1987. Changes in magma composition at Arenal volcano, Costa Rica, 1968–1985: real-time monitoring of open-system differentiation. Bull. Volcanol. 49, 415–434.

Rocchi, S., Armienti, P., D'Osazio, M., Wijbrans, J., Di Vincenzo, G., 2002. Cenozoic magmatism in the western Ross Embayment: role of mantle plume versus plate dynamics in the development of the West Antarctic Rift System. J. Geophys. Res. 107 (B9), 2195, doi:10.1029/2001JB000515.

Rocholl, A., Stein, M., Molzahn, M., Hart, S.R., Worner, G., 1995. Geochemical evolution of rift magmas by progressive tapping of a stratified mantle source beneath the Ross Rift, Antarctica. Earth Planet. Sci. Lett. 131, 207–224.

Ryan, G.R., Kyle, P.R., 2004. Lithium abundance and lithium isotope variations on mantle sources: insights from intraplate volcanic rocks from Ross Island and Marie Byrd Land (Antarctica) and other oceanic islands. Chem. Geol. 212, 125–142.

Saal, A.E., Hart, S.R., Shimizu, N., Hauri, E.H., Layne, G.D., 1998. Pb isotopic variability in melt inclusions from oceanic island basalts, Polynesia. Science 282, 1481–1484.

Salters, V.J.M., Stracke, A., 2004. Composition of the depleted mantle. Geochem. Geophys. Geosyst. 5, Q05B07, doi:10.1029/2003GC000597.

Sims, K.W.W., Hart, S.R., 2006. Comparison of Th, Sr, Nd and Pb isotopes in oceanic basalts: implications for mantle heterogeneity and magma genesis. Earth Planet. Sci. Lett. 245, 743–761.

Sims, K.W.W., Pichat, S., Gauthier, P.-J., Reagan, M.K., Kyle, P.R., Blichert–Toft, J., Dunbar, N., Blusztajn, J., Ball, L., Andrews, J., Layne, G., Charrette, M., 2007-this volume. Constraints on the timescales of magma genesis and evolution at Mt Erebus Antarctica: Constraints from $^{238}U–^{230}Th–^{226}Ra–^{210}Pb$, $^{232}Th–^{228}Ra$ and $^{235}U–^{231}Pa–^{227}Ac$. Journ. Vol. Geotherm Res. doi: 10.1016/j.volgeores.2007.08.006.

Stracke, A., Bizimis, M., Salters, V.J.M., 2003. Recycling oceanic crust: quantitative constraints. Geochem. Geophys. Geosyst. 4 (3), 8003, doi:10.1029/2001GC000223.

Stracke, A., Hofmann, A., Hart, S.R., 2005. FOZO, HIMU, and the rest of the mantle zoo. Geochem. Geophys. Geosyst. 6 (5), QO5007, doi:10.1029/2004GC000824.

Stuckless, J.S., Ericksen, R.L., 1976. Strontium isotopic geochemistry of the volcanic rocks and associated megacrysts and inclusions from Ross Island and vicinity, Antarctica. Contrib. Mineral. Petrol. 58, 111–126.

Sun, S.-S., Hanson, G.N., 1975. Origin of Ross Island basanitoids and limitations upon the heterogeneity of mantle sources for alkali basalts and nephelinites. Contrib. Mineral. Petrol. 54, 139–155.

Todt, W., Cliff, R.A., Hanser, A., Hofmann, A.W., 1996. Evaluation of a $^{202}Pb–^{205}Pb$ double spike for high-precision lead isotope analysis. In: Hart, S.R., Basu, A. (Eds.), Earth processes reading the isotopic code. AGU, vol. 95, pp. 429–437.

Watson, T., Nyblade, A., Wiens, D.A., Anandakrishnan, S., Benoit, M., Shore, P.J., Voigt, D., VanDecar, J., 2006. P and S velocity structure of the upper mantle beneath the Transantarctic Mountains, East Antarctic craton, and Ross Sea from travel time tomography. Geochem. Geophys. Geosyst. 7 (7), Q07005, doi:10.1029/2005GC001238.

White, W.M., Albarède, F., Télouk, P., 2000. High-precision analysis of Pb isotope ratios using multi-collector ICP-MS. Chem. Geol. 16, 257–270.

Workman, R.K., Hart, S.R., 2005. Major and trace element composition of the depleted MORB mantle (DMM). Earth Planet. Sci. Lett. 231, 53–72.

Workman, R.K., Hart, S.R., Jackson, M., Regelous, M., Farley, K.A., Blusztajn, J., Kurz, M., Staudigel, H., 2004. Recycled metasomatized lithosphere as the origin of the enriched mantle II (EM2) end-member: evidence from the Samoan volcanic chain. Geochem. Geophys. Geosyst. 5, Q04008.

Worner, G., 1999. Lithospheric dynamics and mantle sources of alkaline magmatism of the Cenozoic West Antarctic Rift System. Glob. Planet. Change 23, 61–77.

Zindler, A., Hart, S.R., 1986. Chemical geodynamics. Annu. Rev. Earth Planet. Sci. 14, 493–571.

Zreda-Gostynska, G., Kyle, P.R., Finnegan, D., Prestbo, K.M., 1997. Volcanic gas emissions from Mount Erebus and their impact on the Antarctic environment. J. Geophys. Res. 102 (B7), 15039–15055.